

Crushed Stone Utilization in replacing Silica Sand in Ultra-High Performance Concrete

Sang Ngoc Pham

Faculty of Transportation Engineering, Ho Chi Minh City University of Transport, Ho Chi Minh City, Vietnam
phamngocsang@ut.edu.vn

Hung Dinh Nguyen

Faculty of Civil Engineering, Vietnamese-German University, Binh Duong, Vietnam
hung.nd2@vgu.edu.vn

Mai Luu

Faculty of Transportation Engineering, Ho Chi Minh City University of Transport, Ho Chi Minh City, Vietnam
luu.mai@ut.edu.vn (corresponding author)

Received: 16 December 2024 | Revised: 22 January 2025 and 25 January 2025 | Accepted: 27 January 2025

Licensed under a CC-BY 4.0 license | Copyright (c) by the authors | DOI: <https://doi.org/10.48084/etasr.9954>

ABSTRACT

Ultra-High Performance Concrete (UHPC) offers superior load-bearing capacity and durability, yet its reliance on natural Silica Sand (SS) contributes to high production costs and environmental concerns. This study examines the feasibility of substituting SS with Crushed Stone (CS) aggregates in UHPC production. Through a combination of theoretical analysis and experimental investigation, an optimal mixture is identified, and the effects of CS aggregates on key UHPC properties, including flowability, air bubble content, and compressive strength, are evaluated. The experimental results indicate that UHPC incorporating CS aggregates achieves compressive strengths exceeding 130 MPa at 28 days. The Scanning Electron Microscopy (SEM) analysis reveals that the Interfacial Transition Zone (ITZ) surrounding CS aggregates exhibits lower local stiffness due to the predominance of calcium hydroxide (CH) and ettringite crystals. Furthermore, the microstructural analysis identifies the presence of elongated particles (accounting for up to 32% of the mixture) and microcracks within the CS aggregates, which contribute to a reduction in compressive strength. Consequently, UHPC produced with CS aggregates achieves approximately 84% of the compressive strength of UHPC utilizing SS aggregates. Despite this reduction in mechanical performance, the cost-effectiveness of CS-based UHPC is significantly superior, with a 29% reduction in the overall production costs and a 16% improvement in the cost-to-performance ratio compared to SS-based UHPC. These findings demonstrate that CS aggregates provide a viable and economically advantageous alternative to SS in UHPC production, offering significant cost savings while maintaining the essential mechanical properties required for structural applications.

Keywords-UHPC; crushed stone; silica sand; compression strength; microstructure; interracial transition zone

I. INTRODUCTION

UHPC represents one of the most advanced innovations in concrete technology, offering superior mechanical properties and durability compared to Normal-Strength Concrete (NSC) and High-Strength Concrete (HSC). Typically, UHPC exhibits a compressive strength ranging from 120 MPa to 200 MPa, a flexural strength from 8 MPa to 30 MPa, and an elastic modulus from 40 GPa to 55 GPa [1]. In Vietnam, UHPC is commonly produced using materials, such as SS, Silica Powder (QP), Silica Fume (SF), Cement (C), reinforcing fibers, and Superplasticizers (SPs) to reduce the Water-to-Cement (W/C)

ratio. The mixture design follows the principle of microstructural void filling to achieve maximum density [2]. With the available materials and technology, UHPC produced in Vietnam typically attains a compressive strength exceeding 120 MPa. SS is widely used as an aggregate in UHPC due to its advantageous properties. Its varied particle sizes and angular shape help minimize the ITZ, thereby significantly enhancing mechanical strength. However, the use of SS presents several challenges, including high cost, limited availability, and environmentally detrimental extraction practices. Consequently, exploring CS as a viable replacement for SS in UHPC production is crucial. Additionally, optimizing the mix

composition is essential to ensure the desired performance while reducing the construction costs and mitigating the environmental impact. CS is obtained through the mechanical crushing of large rock masses. Therefore, its properties depend on the characteristics of the parent rock, including chemical composition, mineral content, petrographic classification, specific gravity, hardness, strength, physical and chemical stability, pore structure, and color. However, the crushing process alters certain aggregate properties, such as the particle shape, size distribution, surface texture, and moisture absorption. These changes are influenced by factors, involving the rock stratification, crushing method, machinery type, and the sieve hole ratio in the rock grinder. All these factors play a critical role in determining the performance of both fresh and hardened UHPC. The application of CS in concrete mixtures has been extensively studied both domestically and internationally. Its utilization as an aggregate increases the porosity of concrete mixtures due to the high proportion of elongated particles, which contribute to a higher void content compared to SS [3]. This void content further increases based on the properties of the parent rock and the CS production process. To maintain the density of the mineral components and ensure the workability of the concrete mixtures, it is imperative to design and adjust the mixtures appropriately. This ensures that the mixtures meet the desired properties, such as slump flow, durability and strength. In Vietnam, CS is extensively used in construction, following the ASTM C33/C33M standard specification for concrete aggregates [4]. The research and application of CS in NSC and HSC have been relatively comprehensive. However, the use of CS in UHPC remains underexplored both in Vietnam and globally. Limited studies, such as [5], have investigated the influence of different CS, while the existing codes only provide brief requirements for fine aggregates [6]. This research indicated that the hygroscopicity of the CS aggregates is greater, leading to an increased water demand compared to the traditional sand aggregates. NSC can be produced with compressive strengths in the range of 30 MPa to 40 MPa, although the hydrated C layer and transition zone around the aggregate remain relatively weak. Authors in [7] discussed the influence of increasing the fine particle content mass from 1.0% to 5.0% in limestone aggregate on the fresh and hardened properties of HSC. A significant number of experiments considered different aggregate sources, C types, and W/C ratios. The results demonstrated that while increasing the fine particle content slightly reduced fluidity, this could be compensated by adjusting the SP dosage within a realistic range, such as 10%. Other properties, including the air content, compressive strength, and elastic modulus, were not significantly affected. It was concluded that the effect of increasing the fine particle content in crushed limestone aggregate was negligible, allowing its use with only a simple confirmation test of the typical concrete properties. Authors in [8] examined the use of CS in concrete, focusing on the influence of coarse aggregates from various mineralogical sources. The results demonstrated that HSC, with compressive strengths around 70 MPa could be achieved. In [9], based on the production of UHPC from CS, authors optimized the UHPC compositions using aggregates of SS and basalt CS. They determined the optimal mix proportions for UHPC, corresponding to the highest self-

flowability and lowest plastic viscosity. Four different series of self-compacting UHPC, compressive strengths exceeding 190 MPa, were developed with different maximum grain sizes of 1 mm, 2.5 mm, 4 mm, and 8 mm. In [10], the effect of compactness optimization on the performance and durability of UHPC was investigated, utilizing CS to achieve compressive strengths exceeding 200 MPa. Similarly, authors in [11] examined the combination of two coarse basalt aggregates, with a fineness modulus of 3.66 and 4.6 respectively, and SS by optimizing the mixed density. The three mixtures using SS and crushed aggregate with the ratios of 60%, 70%, and 82% in the total aggregate content were tested. The results indicated that the compressive strength of the UHPC specimens reached approximately 150 MPa.

The aforementioned studies have demonstrated that CS can be effectively used in the production of HPC to achieve compressive strengths between 70 MPa and 80 MPa. However, for the production of UHPC with compressive strengths exceeding 120 MPa, the inclusion of SS is generally required. Consequently, producing UHPC utilizing only CS remains a challenge and warrants further comprehensive investigation. This research focuses on concrete mixtures using CS aggregate, with the objective of evaluating the feasibility of this replacement and its impact on the UHPC properties.

II. ASSESSMENT OF THE FEASIBILITY OF TYPES OF CRUSHED STONE AS SUBSTITUTE FOR SILICA SAND IN UHPC MIXTURES

Vietnam's Highlands, Southeast, and Mekong Delta regions have relatively abundant supplies of CS, primarily produced from basalt or granite parent rock. Various crushing plants and size reduction techniques are employed to process these materials. Depending on the intended application, specific requirements for the parent rock strength, mechanical properties, and particle content must be met. Typical CS from the Southeast region -such as Hung Vuong CS, Phu Giao CS, and Fico CS- are derived from parent rock with strengths ranging from 140 MPa to 200 MPa, as depicted in Figure 1. Their fineness modulus ranges from 2.5 to 3, with the aggregate particle content meeting ASTM C33/C33M standards [4]. In this study, Hung Vuong Crushed Stone (CSHV) was utilized for the UHPC production, aiming to achieve compressive strengths exceeding 120 MPa. Additionally, two types of CS from Chau Thoi -Crushed Stone-3 (CS-3) and Crushed Stone-5 (CS-5), derived from basalt parent rock- were utilized as comparative aggregates. These materials were previously used in the UHPC production research in [11]. The fineness modulus of CS-3 and CS-5 is 3.66 and 4.6, respectively, with the particle sizes classified within the coarse aggregate range [4]. Table I presents the properties of these aggregates.

TABLE I. PROPERTIES OF CSHV, CS-3, CS-5, AND SS.

Aggregates	CSHV	CS-3	CS-5	SS
Specific Gravity (g/cm ³)	2.668	2.77	2.72	2.65
Foam Density (g/cm ³)	1.501	1.489	1.521	1.476
Compaction Factor	0.626	0.622	0.609	0.616
Hygroscopicity (%)	0.8	0.7	0.7	0.6
SiO ₂ Content (%)	61.5	60.7	60.7	98.5

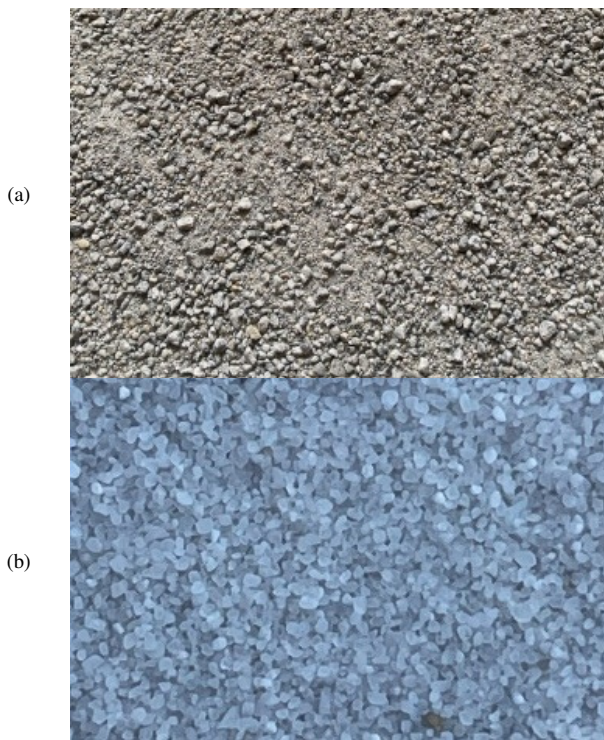


Fig. 1. (a) CS from the southeast regions of Vietnam, (b) SS.

The particle content of CS-3, CS-5, CSHV, and SS was analyzed, as portrayed in Table II and Figure 2. To assess the effect of CS-3 and CS-5 aggregate sizes on the continuity of the grain size distribution in the mixture, previous studies, namely [9-11], were examined. The findings from [11] indicate that both CS-3 and CS-5 fall within the coarse aggregate range, as defined by ASTM C33/C33M [4]. CS-3 has a particle size distribution ranging from 0.3 mm to 5 mm, while CS-5 ranges from 1.18 mm to 5 mm. In contrast, QP exhibits a much finer particle size distribution, ranging from 1 μm to 100 μm.

TABLE II. AGGREGATES PARTICLE CONTENT AND FINENESS MODULUS

Sieve Size	Percent Passing of Aggregates				Requirements	
	CSHV	CS-3	CS-5	SS	[4]	
(mm)	(%)	(%)	(%)	(%)	Min	Max
4.75	99.7	97.5	96.96	100	100	95
2.36	79.98	63.8	30.72	100	100	80
1.18	62.35	39.4	9.04	99.4	85	50
0.6	46.91	21	0	48.4	60	25
0.3	33.47	0.54	0	0.54	30	10
0.15	16.93	0	0	0.24	10	2
0.075	5.23	0	0	0	5	0
< 0.075	0	0	0	0	-	-
Fineness Modulus	2.6	3.66	4.6	2.51		
Shape	Angular			Rounded		
Surface Texture	Crystalline			Smooth		

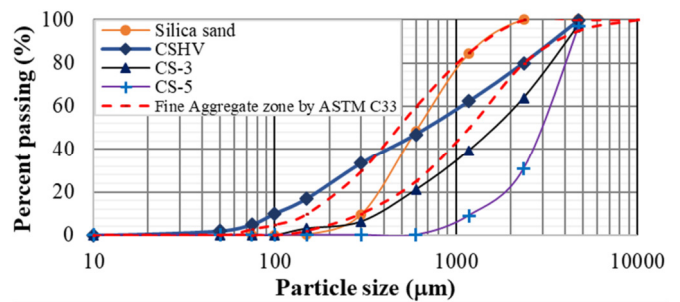


Fig. 2. Passing percentage versus particle size for all aggregates.

When mixing CS-3 and CS-5 with finer particles, such as QP, the aggregate gradation curves exhibit interruptions. This occurs because the minimum particle sizes of CS-3 (0.3 mm) and CS-5 (1.18 mm) are significantly larger than the maximum particle size of QP (0.1 mm). As a result, discontinuities arise in the grain size distribution -specifically in the 0.1 mm to 0.3 mm range for CS-3 and the 0.1 mm to 1.18 mm range for CS-5. To address this issue, authors in [11] utilized SS with particle sizes ranging from 0.14 mm to 1.25 mm to create a more continuous aggregate size distribution. Similarly, other studies [9-10, 18] also incorporated SS as a key aggregate component in UHPC mixtures to optimize the particle gradation.

Table II shows that CSHV consists of particle sizes ranging from 0.075 mm to 5 mm. As illustrated in Figure 2, the aggregate particle distribution curve of CSHV closely aligns with that of SS, predominantly falling within the fine aggregate range as defined by ASTM C33/C33M [4]. The fineness modulus of CSHV is 2.60, which is comparable to that of SS (2.51). Additionally, CSHV and SS exhibit similar characteristics in terms of the particle content, fineness modulus, and physical-mechanical properties. These similarities suggest that CSHV can effectively replace SS in achieving a continuous grain size distribution when combined with SS, using CSHV as a complete substitute for SS in UHPC production.

III. EXPERIMENTAL DETERMINATION OF THE OPTIMAL CONCRETE MIXTURE

A. Materials

In addition to the CSHV, the other materials used in the UHPC mix design are summarized in Table III.

TABLE III. COMPONENTS OF MATERIALS

No.	Constituent	Symbol	Grain Size (μm)	Specific Weight (kg)
1	Cement	C	1-75	3050
2	Silica Fume	SF	0.05-1	2220
3	Silica Powder	QP	1-100	2630
4	Silica Sand	SS	$(0.14-1.25) \times 10^3$	2650
5	Crushed Stone	CS	$(0.075-5) \times 10^3$	2668
6	Water	W	-	1000
7	Superplasticizer	SP	-	1100

The particle distribution of these materials is illustrated in Figure 3, where the vertical axis represents the particle quantity and the horizontal axis represents the particle size, ranging from 0.01 μm to 5000 μm. Based on the UHPC aggregate gradation data in Table III and Figure 3, SF has a maximum

particle size of 1 μm, followed by C, which ranges from 1 μm to 75 μm, and QP, with a range of 1 μm to 100 μm. In contrast, CS exhibits a particle size distribution from 75 μm to 5 mm, forming a continuous gradation with the other fine materials. As a result, the particle content of all components follows a continuous distribution curve, spanning from the smallest particle size of 0.05 μm to the largest at 5 mm.

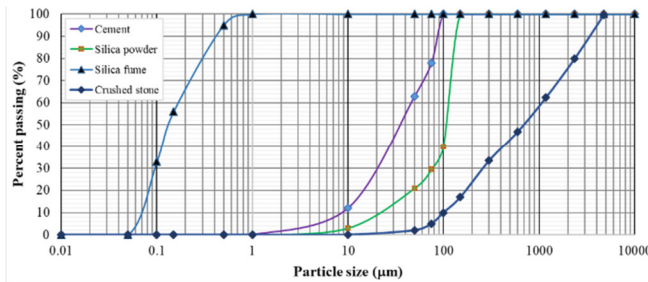


Fig. 3. Particle content chart of all components.

B. Identification of Variables in the Experimental Planning Problem

The current study adapts widely used UHPC formulations of M2Q, M2Qb, and M3Q, proposed in [12], to suit the local material conditions in Vietnam, aiming to identify the optimal mixture for these conditions. The research involved experiments on nine different mixtures, each varying three key parameters: W/C ratio ($x = W/C$), Superplasticizer-to-Cement (SP/C) ratio ($y = SP/C$), and Crushed Stone-to-Cement (CS/C) ratio ($z = CS/C$). The selection of these parameters is based on the following considerations:

1) Water Content

The concrete mixtures M2Q, M2Qb, and M3Q have W/C ratios of 0.22, 0.22, and 0.255, respectively [12]. ACI 211.4R [13] recommends that the W/C ratio should range from 0.22 to 0.34. Therefore, in this study, the variable ratio was selected to range from 0.22 to 0.255. However, due to the higher moisture absorption of CS compared to SS, the selected values were

increased by 0.5%, resulting in trial ratios of 0.225, 0.238, and 0.26.

2) Superplasticizer Content

The polycarboxylate SP employed in this study, which is Sika ViscoCrete-8168, adheres to the surface of fine particles, keeping them separated during hydration. The SP content was selected based on the manufacturer's recommendations and laboratory testing, and ranged from 1.9% to 3.0%.

3) Crushed Stone Content

The fine particle concrete mixtures M2Q, M2Qb, and M3Q have CS/C ratios of 1.17, 1.17, and 1.22, respectively [12]. According to [14], these ratios typically varied from 1.02 to 1.2. For this study, the ratio was selected to be between 1 and 1.2. Therefore, the CS/C ratio selected for the experiments was 1.0, 1.1, and 1.2.

4) Experimental Program

Based on the variations in the selected factors, nine mixtures were analyzed and categorized into three groups, as illustrated in Table IV, based on the CS/C ratio (1.0, 1.1, 1.2). The details of these groups are:

- C1 group (CS/C = 1.0): Includes CP₁, CP₄, and CP₇, with W/C ratios of 0.238, 0.225, and 0.26, and SP/C ratios of 2%, 2.8%, and 1.9%, respectively.
- C2 group (CS/C = 1.1): Includes CP₂, CP₅, CP₈, with W/C ratios of 0.238, 0.225, and 0.26, and SP/C ratios of 2.2%, 3% and 2.1%, respectively.
- C3 group (CS/C = 1.2) Includes CP₃, CP₆, CP₉, with W/C ratios of 0.238, 0.225, and 0.26, and SP/C ratios of 2.5%, 3%, and 2.3%, respectively.

From these groups, the aggregate gradation is established in this study.

5) Concrete Mixtures Testing

Nine mixtures were prepared for experimental evaluation, as presented in Table IV.

TABLE IV. THE PROPOSED COMPOSITION OF CONCRETE MIXTURES

Materials	CP ₁ (kg)	CP ₂ (kg)	CP ₃ (kg)	CP ₄ (kg)	CP ₅ (kg)	CP ₆ (kg)	CP ₇ (kg)	CP ₈ (kg)	CP ₉ (kg)
Water	202	202	202	191	191	191	221	221	221
C	850	850	850	850	850	850	850	850	850
SF	170	170	170	170	170	170	170	170	170
SP	17.00	18.70	21.46	23.80	25.50	25.50	16.15	17.85	19.55
QP	200	200	200	200	200	200	200	200	200
CS	850	946	1037	850	946	1037	850	946	1037
Steel Fibers	78.5	78.5	78.5	78.5	78.5	78.5	78.5	78.5	78.5
W/C Ratio	0.238	0.238	0.238	0.225	0.225	0.225	0.26	0.26	0.26
SP/C Ratio	2.0%	2.2%	2.5%	2.8%	3.0%	3.0%	1.9%	2.1%	2.3%
Density (kg/m ³)	2368	2465	2559	2339	2436	2528	2386	2483	2576

According to [15], the amount of grain passing through the sieve holes can be expressed as:

$$p = 100 \times \left(\frac{d}{D}\right)^n \tag{1}$$

where d is any grain diameter, D is the maximum grain size in the mixture, n is an exponent depending on the grain properties, which, in this study, is equal to 0.26.

Equation (1) accounts for the particle sizes of the materials listed in Table III, with $d = 0.5$ mm and $D = d_{max} = 5$ mm. By applying (1), the theoretical grain mix curve is established

based on the guidelines outlined in [15]. The aggregate distribution of the C1, C2, and C3 mixtures is determined by analyzing the relationship between the cumulative percentage passing through the sieve and the particle diameter, as exhibited in Figure 4.

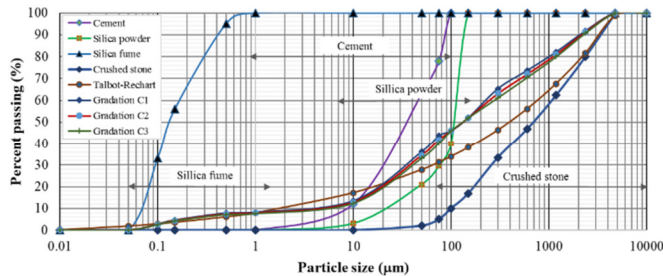


Fig. 4. Particle content chart of the concrete mixture.

A comparison of the particle size distribution curves with the ideal aggregate curves indicates that the particle size distribution follows the theoretical equations of [15]. The aggregates selected for the experimental study are detailed in Table IV, including a steel fiber content of 1%, a diameter of 0.20 mm, a length of 13 mm, an aspect ratio of 65, and a tensile strength of 2800 MPa. To determine the compressive strength of the concrete, this study produced 65 cylindrical specimens with dimensions of 100 × 200 mm, according to ASTM C39/C39M [16]. The specimens were labeled CPi.i.j.k, where i represents the aggregate type, j denotes the model's name within the aggregate type, and k corresponds to the casting time, as shown in Table V. A four-level forced mixer was used to mix the concrete in the laboratory, as displayed in Figure 5.



Fig. 5. Four-level forced mixing equipment.

C. Ultra-High Performance Concrete Mixing Process

The UHPC mixing process consists of the following steps:

- Dry Mixing: Add the powder mixture of C, CS, and SF into the mixer and mix at low speed for 30 seconds.
- Initial Wet Mixing: Add 80% of the water, mix for 30 to 60 seconds at low speed, then add 70-80% of the SP. Mix for

2-3 minutes, checking consistency and adjusting the remaining SP and water until the mixture reaches the desired fluidity. Gradually increase to medium speed.

- Aggregate Incorporation: Add CS and mix for 1-2 minutes, increasing speed from low to medium.
- Final Mixing: Add steel fibers for uniform dispersion, mixing for up to 1 minute to complete the process.

The total mixing time ranged from 5 to 8 min. The fresh concrete was then poured into 65 cylindrical molds (100 × 200 mm), as presented in Figure 6.

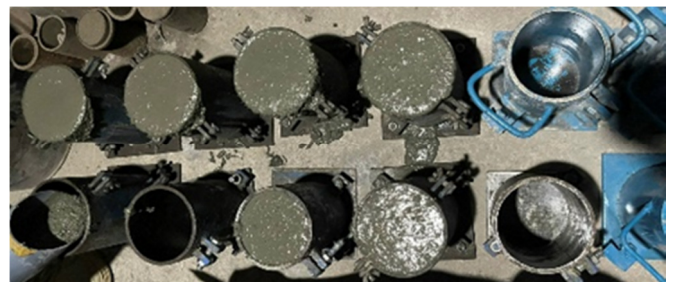


Fig. 6. Concrete pouring into the cylindrical molds.

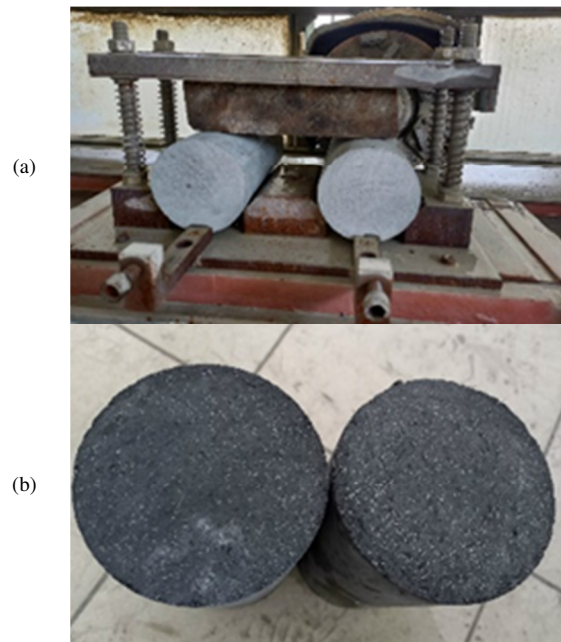


Fig. 7. (a)Specimens grinding, (b)specimens after flat grinding.

To ensure accurate test results, the cylindrical specimens must be compacted and free of warping. The sampling process aimed to minimize the air bubbles in the specimens. After sampling, the surface of the specimens was covered to prevent moisture loss, and they were kept in a natural environment for 24 hours. The specimens then underwent thermal curing for 48 hours before being submerged in water until the designated testing time. Before testing, the specimens' surfaces were flattened using a dedicated grinder to ensure uniform compression, as illustrated in Figure 7.

TABLE V. EXPERIMENTAL RESULTS OF CONCRETE

No.	Mixtures	Specimen ID	Compressive Strength (MPa)	
			Measured	Mean
1	CP1	CP1.1.1.284	110.73	109.78
2	CP1	CP1.1.2.284	112.92	
3	CP1	CP1.1.3.284	110.99	
4	CP1	CP1.1.4.284	104.22	
5	CP1	CP1.1.5.284	110.04	
6	CP2	CP2.2.1.284	127.53	131.74
7	CP2	CP2.2.1.294	130.03	
8	CP2	CP2.2.2.284	124.07	
9	CP2	CP2.2.2.294	132.21	
10	CP2	CP2.2.3.284	129.46	
11	CP2	CP2.2.4.284	131.96	
12	CP2	CP2.2.5.284	133.34	
13	CP2	CP2.2.6.284	141.64	
14	CP2	CP2.2.7.284	135.45	106.61
15	CP3	CP3.3.1.284	106.97	
16	CP3	CP3.3.1.294	102.22	
17	CP3	CP3.3.2.284	117.58	
18	CP3	CP3.3.2.294	101.33	
19	CP3	CP3.3.3.284	113.43	
20	CP3	CP3.3.3.294	104.18	
21	CP3	CP3.3.4.284	117.11	
22	CP3	CP3.3.4.294	100.48	
23	CP3	CP3.3.5.284	101.49	
24	CP3	CP3.3.5.294	99.89	
25	CP3	CP3.3.6.284	119.74	
26	CP3	CP3.3.6.294	103.11	
27	CP3	CP3.3.7.294	98.45	109.48
28	CP4	CP4.4.1.294	113.28	
29	CP4	CP4.4.1.284	107.87	
30	CP4	CP4.4.2.294	113.55	
31	CP4	CP4.4.2.284	102.34	
32	CP4	CP4.4.3.284	104.21	
33	CP4	CP4.4.4.294	127.02	
34	CP4	CP4.4.4.284	103.11	
35	CP4	CP4.4.5.284	106.34	
36	CP4	CP4.4.5.294	125.22	
37	CP4	CP4.4.6.284	101.23	
38	CP4	CP4.4.7.284	100.14	
39	CP5	CP5.5.1.284	123.33	125.20
40	CP5	CP5.5.1.294	128.66	
41	CP5	CP5.5.2.284	130.11	
42	CP5	CP5.5.2.294	137.22	
43	CP5	CP5.5.3.284	113.48	
44	CP5	CP5.5.3.294	126.73	
45	CP5	CP5.5.4.284	116.01	
46	CP5	CP5.5.4.294	128.32	
47	CP5	CP5.5.5.284	119.13	102.09
48	CP5	CP5.5.5.294	129.04	
49	CP6	CP6.6.1.284	100.67	
50	CP6	CP6.6.2.284	100.06	112.30
51	CP6	CP6.6.3.294	102.01	
52	CP6	CP6.6.4.284	105.61	
53	CP7	CP7.7.1.284	110.21	125.86
54	CP7	CP7.7.2.284	108.43	
55	CP7	CP7.7.3.284	114.05	
56	CP7	CP7.7.4.284	116.52	
57	CP8	CP8.8.1.284	122.57	104.42
58	CP8	CP8.8.2.284	128.80	
59	CP8	CP8.8.3.284	125.47	
60	CP8	CP8.8.4.284	127.36	109.24
61	CP8	CP8.8.5.284	125.10	
62	CP9	CP9.9.1.284	102.58	
63	CP9	CP9.9.2.284	105.53	
64	CP9	CP9.9.3.284	109.24	

After curing and surface grinding, the specimens were tested for compressive strength, as depicted in Figure 8.

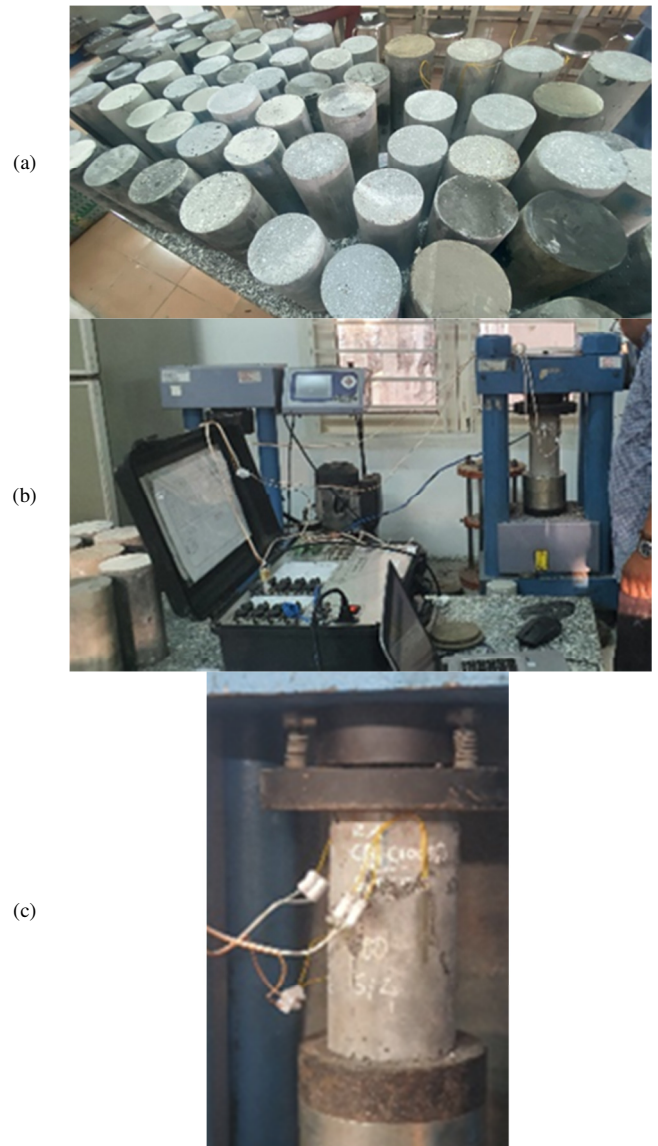


Fig. 8. (a)Preparation of experimental specimens, (b) specimen compression experiments, (c) failure specimens.

IV. REGRESSION ANALYSIS OF CONCRETE STRENGTH

To evaluate the reliability and influence of various factors on the compressive strength of UHPC using CS, the Statistica Package for the Social Sciences (SPSS) software was employed. The third order polynomial regression equation was formulated using the independent variables x, y, z , as expressed in:

$$\begin{aligned}
 R = & \beta_0 + \beta_1x + \beta_2y + \beta_3z + \beta_4xy + \beta_5yz + \beta_6zx \\
 & + \beta_7x^2y + \beta_8y^2z + \beta_9z^2x + \beta_{10}xy^2 + \beta_{11}yz^2 + \\
 & \beta_{12}zx^2 + \beta_{13}x^3 + \beta_{14}y^3 + \beta_{15}z^3 + \beta_{16}xyz
 \end{aligned}
 \tag{2}$$

where β_i represents the regression coefficients, and R represents the compressive strength of UHPC with CS.

A partial F-test, T-test and significance level analysis were conducted in SPSS utilizing the experimental data outlined in Table VI. The results indicate that among the regression coefficients, only certain terms exhibit a significance probability (Sig.) of less than 0.05. Thus, (2) is simplified to:

$$R = \beta_0 + \beta_1 x^2 y + \beta_2 z + \beta_3 z^3 \quad (3)$$

where the variables include the interaction effect between water and SP $x^2 y$, CS content z , and the third order effect of the CS content z^3 . The results of the coefficients β_0 , β_3 , β_7 , and β_{15} are obtained from the SPSS program, as shown in Table VI, and then (3) can be rewritten as:

$$R = -1175.342 - 144.200x^2 y + 1791.926z - 487.032z^3 \quad (4)$$

TABLE VI. REGRESSION COEFFICIENTS

Model	Unstandardized Coefficient	Standardized Coefficient	Significance Level (Sig.)
Constant	-1175.342	-	0.000
$x^2 y$	-144.200	-0.142	0.043
z	1791.926	13.240	0.000
z^3	-487.032	-13.380	0.000

The experimental design yielded a regression equation that characterized the relationship between the compressive strength target function and the influencing factors, water, SP, and CS, as presented in (4). The variables x , y , and z range:

$$\begin{aligned} 0.225 \leq x \leq 0.26 \\ 1.9 \leq y \leq 3 \\ 1 \leq z \leq 1.2 \end{aligned} \quad (5)$$

To simplify the optimization process, let:

$$P(x, y) = -1175.342 - 144.200x^2 y \quad (6)$$

$$Q(z) = 1791.926z - 487.032z^3 \quad (7)$$

Thus, (4) is rewritten as:

$$R = R(x, y, z) = P(x, y) + Q(z) \quad (8)$$

Now, let $t = x^2 y$ and substitute t into (5) and (6):

$$0.225^2 \times 1.9 \leq t \leq 0.26^2 \times 3 \Leftrightarrow 0.0961875 \leq t \leq 0.208$$

$$P(t) = -1175.342 - 144.200t$$

Then, the maximum $P(t)$ is obtained:

$$\begin{aligned} P(t)_{\max} &= -1175.342 - 144.2 \times 0.0961875 \\ &= -1189.21 \end{aligned} \quad (9)$$

Similarly, the maximum of $Q(z)$ can be obtained by differentiating the function of $Q(z)$ with respect to z :

$$Q'(z) = 1791.926 - 1461.096z^2$$

$$Q'(z) = 0 \Leftrightarrow z_0 = 1.10744$$

$$Q'(z_0) = -2922.192 \times 1.10744 = -3236.152 < 0$$

Thus, $Q(z)$ reaches a maximum at z_0 :

$$\begin{aligned} Q(z)_{\max} &= 1791.926 \times 1.10744 - 487.032 \times 1.10744^3 \\ &= 1322.97 \end{aligned} \quad (10)$$

Finally, the maximum value of R can be obtained as:

$$R_{\max} = -1189.21 + 1322.97 = 133.76 \text{ MPa}$$

Corresponding to $t_0=0.0961875$ and $z_0=1.10744$, the optimal variable values are $x_0 = 0.225$, $y_0 = 1.9$, and $z_0 = 1.10744$.

The compressive strength test results, listed in Table V, indicated that the CP2.2.5.284 specimen achieved a compressive strength of 133.34 MPa, which is approximately equal to the predicted maximum strength R_{\max} . Additionally, the compressive strengths of CP2.2.7.284 (135.45 MPa), CP2.2.2.294 (132.21 MPa), and CP2.2.2.294 (131.74 MPa) also closely match the expected maximum values. These specimens belong to the CP2 concrete mixture, which corresponds to the following optimal mix proportions: $W/C = 0.238$, $SP/C=2.2\%$, $CS/C = 1.2$. Therefore, in this study, the CP2 concrete mixture with these ratios is identified as the optimal concrete mix for UHPC using CS. The results also demonstrated that reducing the amount of water and SP within a certain range increased the compressive strength. However, this achievement is not solely dependent on the mixed/mixture proportions; other factors, such as the mixing time and stable flowability must be also optimized. Deviations in the sand content, whether higher or lower than the optimal amount, reduce the compressive strength. This phenomenon is attributed to a decrease in density at points nearer the boundary and a non-optimal particle content compared to the theoretical aggregate gradation curve proposed in [15].

V. PROPERTIES OF ULTRA-HIGH PERFORMANCE CONCRETE WITH OPTIMAL MIXTURE

A. Flowability

Flowability is a crucial parameter for assessing the consistency and workability of a UHPC mixture. After mixing, the fresh concrete was tested for flowability utilizing cone mold. The results, including the slump flow measurements for the specimen groups of the optimal mixture containing CS and SS are presented in Figure 9 and Table VII.

For the control mixture without SS, the slump flow of the mixtures reached 243 mm in a C230 cone and 722 mm in a mini-slump cone. During the experiment, the material distribution was carefully monitored to prevent water separation, stratification, and sedimentation. The flowability was analyzed when CS was mixed with SS while maintaining a constant total mass. The proportion of SS was adjusted to 100%, 50%, and 0%, leading to the following slump flow results: 765 mm/268 mm, 737 mm/255 mm, and 722 mm/243 mm for the mini-slump cone and C230 cone, respectively. Additionally, the air bubble content was measured for each mix, as can be seen in Table VII.

TABLE VII. RESULTS OF THE SLUMP FLOW AND AIR BUBBLE CONTENT TESTING OF THE UHPC MIXTURES

Targets	0% CS	50% CS	100% CS
Slump Flow (Cone C230), mm	268	255	243
Slump Flow (Mini-Slump Cone), mm	765	737	722
Air Bubble Content, %	2.3	2.5	2.6



Fig. 9. (a) Slump flow (mini-slump cone), (b) slump flow of UHPC, (c) slump flow test (C230 cone), (d) slump flow of 100% CS, (e) slump flow of 50% CS, (f) slump flow of 0% CS-100% SS.

The hygroscopic properties of the aggregates, as presented in Table I, indicated that the CSHV aggregates have a hygroscopicity of 0.8, while the SS aggregates have a hygroscopicity of 0.6. As a result, the increase in the CS content leads to higher hygroscopicity, which reduces the overall flowability of the UHPC mixture. However, accurately predicting the exact relationship between the CS content and slump flow reduction remains challenging.

Additionally, as portrayed in Figure 3, the CSHV aggregates contain 5.23% more fine particles than the SS aggregates. This increased fine content affects the slump flow behavior of the mixture. To maintain a slump flow of 240-260 mm, similar to that of the SS aggregates, the SP amount in UHPC mixtures with CS aggregates must be increased by 10%. This is due to the increase in the fine particle content in the CS, which raises the surface area of the aggregates. This, in turn, reduces the available surface slurry, despite a constant slurry phase volume, making it more difficult for the particles to move freely, thus increasing the viscosity of the concrete mixture. To mitigate this, additional water and SP are required to enhance the particle dispersion within the mixture.

B. Comparison of Compressive Characteristics between UHPC with Crushed Stone and UHPC with Silica Sand

The test specimens were initially cured naturally for 24 hours. Following this period, the molds were removed, and the specimens underwent moisture heat at 90°C for a further 48 hours. Finally, the specimens were soaked in water until compression testing. All specimens were subjected to uniaxial compressive loads using a 2000 kN hydraulic jack, with an average loading rate of 0.25 MPa per second. The experimental results are presented in Table VIII and Figure 10. In the current study, the paste phase in the concrete mixtures remains constant, meaning that the differences in compressive strength between the mixtures primarily result from variations in the characteristics of the CS-3, CS-5, CSHV, and SS aggregates. When the optimal mixture exclusively incorporates the CSHV aggregate, the compressive strengths of UHPC at 3 days and 14 days reach 89.22% (115.98 MPa) and 92.05% (119.65 MPa), respectively, relative to the 28-day compressive strength (129.98 MPa). In contrast, the mixtures containing only CS-3 or CS-5 aggregates (without SS) exhibit lower 28-day compressive strengths, achieving 86.75% (112.76 MPa) and 79.79% (103.71 MPa) of the compressive strength observed with the CSHV aggregate, respectively. This reduction can be attributed to the minimum particle sizes of CS-3 (0.3 mm) and CS-5 (1.25 mm), which create discontinuities when mixed with QP particles that have a maximum size of 0.1 mm. To ensure continuous particle size distribution and improve the compressive strength, previous studies recommend incorporating SS as an intermediate aggregate in UHPC mixtures. The results also reveal that UHPC with the CSHV aggregate has an average compressive strength 18.7% lower than that of UHPC with the SS aggregate. This difference is largely due to CSHV being a type of manufactured sand with a maximum particle size of 5 mm, whose particle properties depend on the production technology. Additionally, certain limitations of CSHV contribute to its reduced strength. For instance, 32% of its particles in the 4.75 mm (No. 4) sieve are elongated, as shown in Figure 12(a). Elongated particles are defined as those with a thickness or width less than one-third of their length. Furthermore, some CSHV aggregates exhibit microcracks, as depicted in Figures 11(b) and 12(c), which further contribute to the reduction in compressive strength.

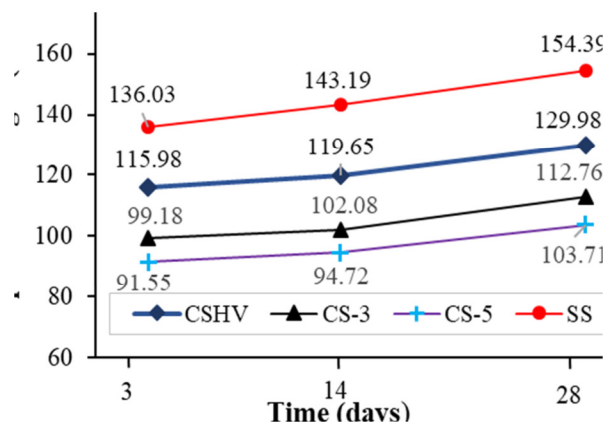


Fig. 10. Compressive strength development chart of UHPC after moisture heat curing.

TABLE VIII. THE COMPRESSIVE STRENGTH OF UHPC WITH CSHV, CS-3, CS-5, AND SS AGGREGATES

Mixtures	Compressive Strength (MPa)								
	Specimen Name	R ₃	R th ₃	Specimen Name	R ₁₄	R th ₁₄	Specimen Name	R ₂₈	R th ₂₈
CSHV	HV.2.1.294	117.02	115.98	HV.2.1.054	120.32	119.65	HV.2.1.284	127.53	129.98
	HV.2.2.294	119.25		HV.2.2.054	111.40		HV.2.2.284	124.07	
	HV.2.3.294	115.36		HV.2.3.054	119.20		HV.2.3.284	119.21	
	HV.2.4.294	119.58		HV.2.4.054	119.83		HV.2.4.284	131.96	
	HV.2.5.294	113.32		HV.2.5.054	124.45		HV.2.6.284	141.64	
	HV.2.6.294	111.36		HV.2.6.054	122.69		HV.2.7.284	135.45	
CS-3	CS3.2.1.294	97.32	99.18	CS3.2.1.304	111.32	102.08	CS3.2.1.015	104.12	112.76
	CS3.2.2.294	102.99		CS3.2.2.304	105.40		CS3.2.2.015	118.35	
	CS3.2.3.294	99.87		CS3.2.3.304	89.32		CS3.2.3.015	112.32	
	CS3.2.4.294	95.35		CS3.2.4.304	107.36		CS3.2.4.015	113.98	
	CS3.2.5.294	105.21		CS3.2.5.304	96.54		CS3.2.6.015	112.13	
	CS3.2.6.294	94.36		CS3.2.6.304	102.56		CS3.2.7.015	115.68	
CS-5	CS5.2.1.294	87.76	91.55	CS5.2.1.304	101.32	94.72	CS5.2.1.015	101.23	103.71
	CS5.2.2.294	98.23		CS5.2.2.304	89.72		CS5.2.2.015	102.34	
	CS5.2.3.294	92.78		CS5.2.3.304	95.51		CS5.2.3.015	95.17	
	CS5.2.4.294	93.54		CS5.2.4.304	89.23		CS5.2.4.015	101.43	
	CS5.2.5.294	87.34		CS5.2.5.304	97.31		CS5.2.6.015	112.64	
	CS5.2.6.294	89.67		CS5.2.6.304	95.23		CS5.2.7.015	109.45	
SS	SS.2.1.294	137.231	136.03	SS.2.1.225	142.12	143.19	SS.2.1.015	167.34	154.39
	SS.2.2.294	134.523		SS.2.2.225	147.88		SS.2.2.015	153.56	
	SS.2.3.294	139.134		SS.2.3.225	139.78		SS.2.3.015	142.75	
	SS.2.4.294	133.623		SS.2.4.225	141.24		SS.2.4.015	152.78	
	SS.2.5.294	135.32		SS.2.5.225	142.35		SS.2.6.015	154.22	
	SS.2.6.294	136.36		SS.2.6.225	145.79		SS.2.7.015	155.67	

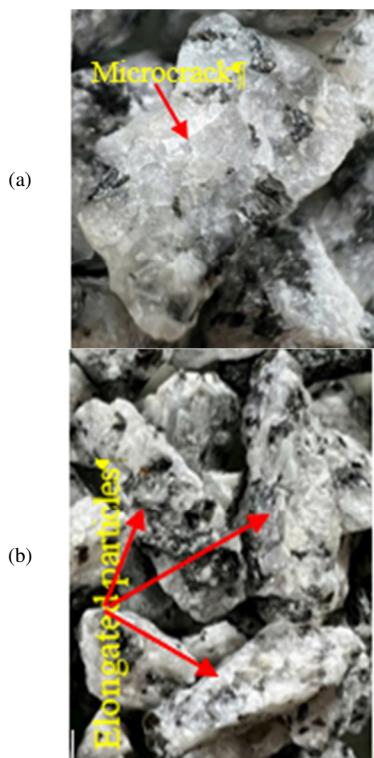


Fig. 11. (a) Microcracks in aggregate particles, (b) elongated aggregate particles.

In the case of the CS aggregates, the wall effect leads to the formation of larger voids around the aggregates/them compared to the SS aggregates. This results in coarser grains filling these voids, ultimately reducing the packing density at the interface. Additionally, the wall effect disrupts the geometric

arrangement of the C and SF particles in the surrounding water, increasing the local W/C ratio. Consequently, this hinders the hydration and pozzolanic reactions in the affected zone.

Consequently, the transition zone around the CS aggregates exhibits lower local stiffness, primarily due to the presence of calcium hydroxide (CH) and ettringite crystals, as demonstrated in Figures 12(e) and 12(f). Moreover, this affected zone is more widely distributed in the CS-based mixtures compared to those with SS aggregates. Based on this analysis, the region surrounding the CS aggregates has lower stiffness and a less dense microstructure than that around the SS aggregates. Additionally, pores and microcracks are present in this area, as depicted in Figure 12(d), which further explains why UHPC with CS aggregates exhibits lower compressive strength than UHPC with SS aggregates.

The results indicate that CSHV, with a particle size range of 0.014 mm to 5 mm, qualifies/is qualified as a fine aggregate according to [4], and follows a continuous particle gradation curve in line with the theoretical model of [15]. This allows for the production of UHPC with a compressive strength reaching 130 MPa without requiring intermediate materials, like SS, which were necessary in previous studies [9-11]. However, despite these advantages, the CSHV aggregates also have certain drawbacks compared to the SS aggregates. These include a high percentage (up to 32%) of elongated particles and the presence of microcracks in some particles, both of which can reduce the overall strength of UHPC.

Furthermore, the larger maximum particle size (5 mm) of CSHV, compared to 1.25 mm in SS, contributes to a weakened ITZ. This explains why UHPC using CSHV aggregates achieves only 84% of the compressive strength attained with SS-based UHPC.

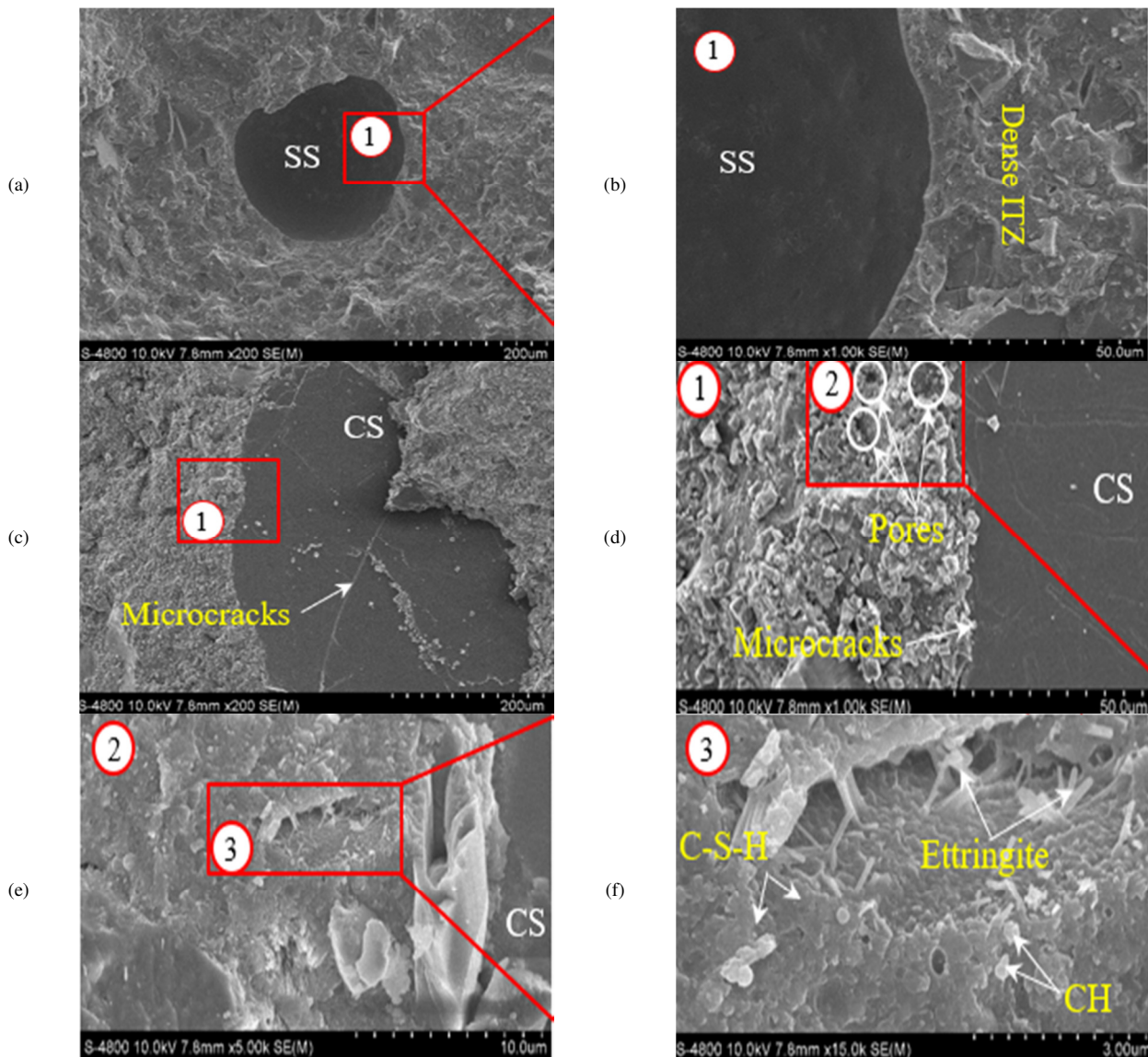


Fig. 12. ITZ of UHPC using SS and UHPC using CSHV: (a) SEM of SS transition zone (200x), (b) SEM of SS transition zone (1000x), (c) SEM of CS transition zone (200x), (d) SEM of CS transition zone (1000x), (e) SEM of CS transition zone (5000x), (f) SEM of CS transition zone (15000x).

In addition, the findings of this study indicate that the compressive strength of UHPC utilizing CSHV aggregates is approximately 87% of that achieved by UHPC with CS, as reported in [11]. In that study, the authors employed a combination of two coarse basalt aggregates, with particle sizes ranging from 0.3 mm to 5 mm for the first group and from 1.18 mm to 5 mm for the second group, along with SS with particle sizes between 0.14 mm and 1.25 mm. Notably, authors in [11] incorporated SS, which is both costly and associated with significant environmental impacts. Authors in [19] investigated two UHPC mixtures. The first mixture was based on G7 formulations and used coarse basalt aggregates with particle sizes ranging from 2 mm to 5 mm, while the second mixture, classified as B4Q, featured particle sizes from 5 mm to 8 mm. Both mixtures utilized CS accounting for 63% of the total aggregate, and incorporated SS as an intermediate aggregate.

These formulations produced UHPC with compressive strengths of up to 150 MPa. Similarly, authors in [20] explored the UHPC properties using solely SS aggregates and combinations of SS with coarse basalt aggregates. The crushed basalt aggregates, with particle sizes between 2 mm and 5 mm, constituted 69% of the total aggregate content. The feasibility of manufacturing UHPC with compressive strengths ranging from 150 MPa to 160 MPa for the mixtures using only SS, and from 150 MPa to 165 MPa for the mixtures using SS and basalt aggregates was demonstrated. Overall, the studies [11, 19, 20] successfully produced UHPC incorporating crushed basalt aggregates and SS. In these studies, SS played a critical role as an intermediate aggregate, enabling the formation of a continuous particle gradation curve when combined with coarser aggregates. This particle gradation, along with the superior properties of SS, significantly enhanced the

microstructure and compressive strength of the hardened UHPC. In contrast, the present study achieved UHPC with compressive strengths exceeding 130 MPa without utilizing SS. Instead, the aggregate mixtures exclusively consisted of CS with particle sizes ranging from 0.075 mm to 5 mm. This demonstrates the potential to develop high-strength UHPC while eliminating the need for SS, offering cost savings and reducing environmental impacts associated with its usage.

VI. EVALUATION OF ULTRA-HIGH PERFORMANCE CONCRETE COST

The high production cost of UHPC remains a significant challenge to its widespread adoption in construction projects. The cost is directly influenced by the material components, with UHPC using CS (UHPC-A) and UHPC using SS (UHPC-B) priced at approximately 6.1 million VND/m³ and 8.7 million VND/m³, respectively, as exhibited in Table IX. The cost distribution for UHPC-A and UHPC-B, depicted in Table X, reveals that the CS aggregate in UHPC-A contributes to 4.64% of the total cost, whereas the SS aggregate in UHPC-B accounts for 32.73%. This substantial difference makes UHPC-A significantly more cost-effective than UHPC-B.

TABLE IX. CALCULATION OF THE COST-COMPRESSIVE STRENGTH RELATIONSHIP FOR 1 M3 OF UHPC

Mixture Sign	Cost (VND)	Cost (USD)*	Compressive Strength (MPa)	Cost/Strength (USD/MPa)
UHPC-A	6.117.820	240	129.98	1.85
UHPC-B	8.672.020	341	154.39	2.21

* (USD 1=VND 25,455.00, current exchange rate on May 2024).

TABLE X. COST RATIOS OF COMPONENTS OF UHPC-A AND UHPC-B

No.	Mixtures	Cost Ratios of Components	
		UHPC-A (%)	UHPC-B (%)
1	Water	0.03	0.23
2	C	41.68	29.40
3	SF	22.23	15.68
4	SP	18.34	12.94
5	QP	13.08	9.23
6	SS	-	32.73
7	CS	4.64	-

As shown in Table IX, UHPC-A is 29% less expensive than UHPC-B overall and 16% more cost-effective when comparing the cost-to-compressive strength ratio. While UHPC-A has a slightly lower compressive strength than UHPC-B, its significantly lower cost makes it the most economical choice. This cost efficiency is primarily due to the substantially lower price of the CS aggregate compared to the SS aggregate. As a result, UHPC incorporating the CS aggregate demonstrates economic efficiency. This study does not compare costs with those of other studies, since raw material prices fluctuate by region and overtime. However, the findings highlight the potential for cost reduction in UHPC production by utilizing CS aggregates instead of SS.

VII. CONCLUSIONS

This study investigates the feasibility of replacing Silica Sand (SS) with the Hung Vuong Crushed Stone (CSHV)

aggregate in Ultra-High Performance Concrete (UHPC). The CSHV aggregate, derived from granite parent rock in the Hung Vuong quarry (Southeast region) was evaluated for its particle content, fineness modulus, and physical-mechanical properties, demonstrating good agreement with those of SS. Unlike the traditional Crushed Stone (CS) categorized as a coarse aggregate, CSHV falls within the fine aggregate range according to ASTM C33/C33M. With a minimum particle size of 0.075 mm, CSHV contributes to a continuous grain size distribution when combined with Silica Powder (QP) (maximum size 0.1 mm) and other fine components. These characteristics confirm the suitability of CSHV as a complete replacement for SS in UHPC production.

A regression equation, derived from the experimental data, describes the influence of CS on UHPC compressive strength. The optimal mixture to achieve 130 MPa compressive strength was determined using the following ratios: Crushed Stone-to-Cement (CS/C) of 1.1, Water-to-Cement (W/C) of 0.238, and Superplasticizer-to-Cement (SP/C) of 2.2. Based on this optimized mixture, the flowability and compressive strength of UHPC incorporating the CS aggregate were investigated, while other properties, such as direct tensile strength, flexural strength, or durability will be addressed in future studies.

The following observations and conclusions can be drawn from the experimental study:

- The CSHV aggregates contain up to 32% elongated particles due to the manufacturing process, leading to fractures occurring primarily within the aggregate at weak points, such as defects and boundaries.
- Microcracks within the CSHV aggregates further contribute to early failure under external forces, often preceding failure within the Interfacial Transition Zone (ITZ) or Cement (C) matrix.
- The Scanning Electron Microscopy (SEM) analysis of ITZs surrounding the CS and SS aggregates revealed that the wall effect in the CS aggregates creates larger voids around the particles.
- These voids are filled by coarser grains, reducing the packing density and consequently weakening the transition zone.
- This phenomenon explains why UHPC with CSHV aggregates reaches only 84% of the compressive strength achieved with UHPC using SS.
- UHPC produced with CSHV aggregates is 29% more cost-effective than UHPC using SS.
- The cost-to-performance ratio improves by 16%, making CSHV-based UHPC a viable alternative without compromising key performance attributes.
- The use of the CS aggregates not only reduces the production costs, but also minimizes the environmental impact by eliminating the need for SS, which is costly and resource-intensive.

Given these technical and economic advantages, further research and wider adoption of the CS aggregates in UHPC production are strongly recommended, particularly in Vietnamese regions rich in CS resources, such as the Highlands, Southeast, and Mekong Delta.

ACKNOWLEDGEMENTS

The authors acknowledge the supports of Hoang Vinh Technical Research and Construction Consulting Company Limited for providing machinery, equipment, and technology during the research process.

REFERENCES

- [1] M. Cornelia, I. Sosa, C. Negrutiu, and B. Hegdes, "Mechanical Properties and Durability of Ultra-High-Performance Concrete," *ACI Materials Journal*, vol. 109, no. 2, 2012, Art. no. 177, <https://doi.org/10.14359/51683704>.
- [2] H. Bahmani and D. Mostofinejad, "Microstructure of ultra-high-performance concrete (UHPC) – A review study," *Journal of Building Engineering*, vol. 50, Jun. 2022, Art. no. 104118, <https://doi.org/10.1016/j.jobee.2022.104118>.
- [3] H. Donza, O. Cabrera, and E. F. Irassar, "High-strength concrete with different fine aggregate," *Cement and Concrete Research*, vol. 32, no. 11, pp. 1755–1761, Nov. 2002, [https://doi.org/10.1016/S0008-8846\(02\)00860-8](https://doi.org/10.1016/S0008-8846(02)00860-8).
- [4] ASTM C33/C33M-16E1, *Standard Specification for Concrete Aggregates*, Feb. 2016.
- [5] P. C. Aitcin and S. Mindess, "High-performance concrete: science and applications," in *Materials Science of Concrete V*, Westerville, OH, USA: American Ceramic Society, 1998, pp. 477–512.
- [6] ACI Committee 363, "State-of-the-Art Report on High-Strength Concrete," Farmington Hills, MI, USA, ACI 363R-92, 1997.
- [7] K. Hayashi, K. Tada, K. Yamada, and H. Kawano, "The Influence of Fine Particle Contents in Limestone Coarse Aggregate on the Properties of High-strength Concrete," *Concrete Journal*, vol. 49, no. 12, pp. 12_31-12_38, Dec. 2011, https://doi.org/10.3151/coj.49.12_31.
- [8] P. C. Aitcin and P. K. Mehta, "Effect of Coarse Aggregate Characteristics on Mechanical Properties of High-Strength Concrete," *Materials Journal*, vol. 87, no. 2, pp. 103–107, Mar. 1990, <https://doi.org/10.14359/1882>.
- [9] H. Kim, P. Hadl, and V. T. Nguyen, "A New Mix Design Method for UHPC based on Stepwise Optimization of Particle Packing Density," *International Interactive Symposium on Ultra-High Performance Concrete*, vol. 1, no. 1, Jul. 2016, <https://doi.org/10.21838/uhpc.2016.66>.
- [10] T. Teichmann and M. Schmidt, "Influence of the packing density of fine particles on structure, strength and durability of UHPC," in *International Symposium on Ultra High Performance Concrete*, Kassel, Germany, Sep. 2003, pp. 465–482, https://doi.org/10.1007/978-3-030-51485-3_31.
- [11] V. T. H. Chu, V. D. Bui, and T. V. Nguyen, "Effect of Combining the Aggregate Grading with Cementitious Composition on Mechanical Properties of Ultra-High Performance Concrete," *Buildings*, vol. 13, no. 1, Jan. 2023, Art. no. 248, <https://doi.org/10.3390/buildings13010248>.
- [12] M. Schmidt, E. Fehling, S. Fröhlich, and J. Thiemicke, "Sustainable building with ultra-high performance concrete—results of the German priority programme 1182 funded by deutsche forschungsgemeinschaft (DFG)," *Structural Materials and Engineering Series; Kassel University Press: Kassel, Germany*, vol. 22, 2014.
- [13] ACI Committee 211, "Guide for Selecting Proportions for High-Strength Concrete Using Portland Cement and Other Cementitious Materials," Farmington Hills, MI, USA, ACI 211.4R-08, Dec. 2008.
- [14] B. A. Graybeal, "Material Property Characterization of Ultra-High Performance Concrete," Research, Development, and Technology Turner-Fairbank Highway Researcher Center, McLean, VA, USA, FHWA-HRT-06-103, Aug. 2006. [Online]. Available: <https://rosap.nhtl.gov/view/dot/38714>.
- [15] A. N. Tailbot and F. E. Richart, *The Strength of Concrete its Relation to the Cement Aggregates and Water*, Urbana, IL, USA: University of Illinois, Oct. 1923.
- [16] *Standard Test Method for Compressive Strength of Cylindrical Concrete Specimens*, ASTM C39/C39M-99, West Conshohocken, PA, USA, 2012.
- [17] J. P. Ollivier, J. C. Maso, and B. Bourdette, "Interfacial transition zone in concrete," *Advanced Cement Based Materials*, vol. 2, no. 1, pp. 30–38, Jan. 1995, [https://doi.org/10.1016/1065-7355\(95\)90037-3](https://doi.org/10.1016/1065-7355(95)90037-3).
- [18] H. D. Nguyen, S. Khatir, and Q. B. Nguyen, "A Novel Method for the Estimation of the Elastic Modulus of Ultra-High Performance Concrete using Vibration Data," *Engineering, Technology & Applied Science Research*, vol. 14, no. 4, pp. 15447–15453, Aug. 2024, <https://doi.org/10.48084/etasr.7859>.
- [19] B. D. Vinh, "Behaviour of Steel-Concrete Composite Beams Made of Ultra High Performance Concrete," PhD dissertation, Economic Sciences, Leipzig University, Leipzig, Germany, 2010.
- [20] J. Ma, M. Orgass, F. Dehn, D. Schmidt, and N. V. Tue, "Comparative Investigations on UltraHigh Performance Concrete with and without Coarse Aggregates," presented at the International Symposium on Ultra High Performance Concrete (UHPC), Kassel, Germany, Sep. 2004, pp. 205-212.